

Cardiovascular Topics

Study of the mechanism of Shexiang Baoxin pill-mediated angiogenesis in acute myocardial infarction

Jingxun Wei, Binchang Dong, Xin Du, Huipu Xu

Abstract

Aim: The Shexiang Baoxin pill (SBP) is a commonly used drug for the treatment of coronary artery disease in China. More recently, some studies have found that it improved coronary microvascular function. This study aimed to explore the possible mechanism by which the SBP promotes angiogenesis after acute myocardial infarction (AMI).

Methods: A rabbit model of acute myocardial infarction was established by ligating the left anterior descending coronary artery with silk thread, and the limb lead electrocardiogram was recorded to determine the success of the model. The rabbits were divided into a control group (SBP + normal rabbit group), a sham operation group, a saline + AMI group and an SBP + AMI group. There were 10 rabbits in each group. The animals were sacrificed and myocardial tissue was collected seven days after the operation. Haematoxylin–eosin staining was used to observe the histological changes in the rabbit myocardium in each group. The degree of acute myocardial infarction was observed with picric acid staining, which was used to detect the expression of vascular endothelial growth factor (VEGF), silent information regulator 1 (SIRT1), Beclin1 and mTOR protein in the myocardial tissue of each group. Immunofluorescence CD31-labelled microvascular density (MVD) was used to observe the vascular regeneration of the rabbits in each group.

Results: Compared with the normal saline + AMI group, the myocardial infarction area of the SBP + AMI group decreased and CD31 immunofluorescence-labelled MVD increased. Compared with the control and sham operation groups, the expression of VEGF, Beclin1 and mTOR in the normal saline + AMI group and the SBP + AMI group increased, while the expression of SIRT1 decreased. Compared with the normal saline + AMI group and the SBP + AMI group, the positive expression of VEGF, Beclin1, mTOR and SIRT1 in the SBP + AMI group was significantly increased.

Conclusion: Autophagy was enhanced after acute myocardial infarction. SBP may affect angiogenesis through the SIRT1/mTOR signalling pathway after acute myocardial infarction to inhibit ventricular remodelling and a decline in cardiac function.

Keywords: Shexiang Baoxin pill, SIRT1, mTOR, autophagy, vascular regeneration

Submitted 30/9/22; accepted 29/5/23

Cardiovasc J Afr 2023; 34: online publication

www.cvja.co.za

DOI: 10.5830/CVJA-2023-030

Acute myocardial infarction is common in cardiovascular medicine. It has an acute onset and rapid progression, which seriously threatens the patient's safety. The key to the treatment of acute myocardial infarction is to restore blood perfusion over time, reduce the infarct area and protect cardiac function as much as possible. However, just opening the blood vessels does not mean that the myocardial tissue can achieve effective blood perfusion, and promoting the formation of new blood vessels can better inhibit ventricular remodelling and the decline of cardiac function.¹ Studies have shown that the collateral circulation of the heart muscle will gradually form after ischaemic injury, but it is too slow to effectively protect cardiac function. Therefore, therapeutic angiogenesis has become a hot research topic.

The Shexiang Baoxin pill (SBP), which consists of seven medicinal materials, including *Cinnamomum cassia*, is widely used as a traditional Chinese patent medicine for the treatment of coronary heart disease. Recent studies have confirmed that the SBP can promote angiogenesis after acute myocardial infarction.^{2,3} However, its mechanism of action remains unclear. Studies have shown that the silent information regulator 1 (SIRT1)/mTOR signalling pathway is involved in the mechanism of angiogenesis after acute myocardial infarction.⁴

The purpose of this study was to explore the possible mechanism of the SBP in promoting angiogenesis after acute myocardial infarction, and provide new ideas and methods for the clinical treatment of acute myocardial infarction.

Methods

Forty male New Zealand white rabbits, two to three months old and weighing 2–2.5 kg, were selected and provided by Jinan Xingkang Biotechnology Co, Ltd. with license no. SCXK (Lu) 20150001. There was indoor feeding, good ventilation, an ambient temperature of approximately 25°C and a relative humidity of approximately 45%. All rabbits were allowed to drink freely and ate three times a day. The experiment was started one week after adaptive feeding.

The feeding of the experimental animals and the operation of animal experiments were reviewed by the ethics committee

Department of Cardiovascology, Department of Internal Medicine, Binzhou Medical University Hospital, Binzhou, PR China

Jingxun Wei, MD

Binchang Dong, MD

Xin Du, MD

Huipu Xu, MD, xuhuipu2022@163.com

of the Affiliated Hospital of Binzhou Medical College and strictly complied with the provisions of the management of experimental animals.

The SBP was purchased from Shanghai Hehuang Pharmaceutical Co, Ltd; mouse anti-human vascular endothelial growth factor (VEGF) (ZM-0265) was purchased from Zhongshan Jinqiao Co, Ltd; Beclin1 (sc-48341), mTOR (sc-517464) and CD31 (sc-376764) antibodies were purchased from Santa Cruz Co, Ltd; SIRT1 (a0018-1) was purchased from Bode Co, Ltd; goat anti-rabbit polyclonal IgG labelled with Alexa Fluor 488 was purchased from Abcam Co, Ltd, UK; and universal secondary antibody and DAB chromogenic solution were purchased from Beijing Zhongshan Jinqiao Co, Ltd.

Before modelling, the experimental animals were fasted for eight hours, weighed before the operation, put in the rabbit box and administered anaesthesia of 10% chloral hydrate intravenous injection at the ear margin at a dose of 3 ml/kg. The rabbits were fixed on a rabbit table. Before the operation, the electrocardiogram (ECG) of the limb leads was recorded using an animal function experimental instrument. A 5-0 surgical suture was used to pass through approximately half of the anterior descending branch of the left coronary artery and ligation was carried out of the anterior descending branch of the left coronary artery. In the sham operation group, sutures were used to pass only through the anterior descending branch without ligation.

After confirmation, the pleural muscle and skin layers were continuously sutured. After chest closure, the ECG was recorded again, showing that the ST-segment of the relevant leads was significantly elevated. There was no significant change in the sham operation group.

The rabbits were randomly divided into four groups, with 10 rabbits in each group, and randomly numbered. A follow-up experiment was carried out after one week of adaptive feeding. The rabbits were divided into the control, sham operation, normal saline + AMI and SBP + AMI groups.

In the control group, the SBP (50 mg/kg, three times a day) was administered by gavage and the rabbits were fed normally. In the sham operation group, only the left anterior descending branch was crossed without ligation, and the rabbits were fed normally. In the normal saline + AMI group, normal saline (50 mg/kg, three times a day) was administered by gavage, and the left anterior descending branch was ligated. The rabbits were fed normally. In the SBP + AMI group, SBP (50 mg/kg, three times a day) was administered by gavage, the left anterior descending branch was ligated and the rabbits were fed normally.

During intragastric administration, we worked gently to avoid damaging the digestive tract of the rabbits. We always observed whether the rabbits vomited the SBP to ensure that it was administered regularly and quantitatively.

On the seventh day after the operation, the rabbits were placed in a rabbit box and fixed. The rabbits were anaesthetised with 10% chloral hydrate. After anaesthesia was successful, the hearts were removed, washed with a large amount of normal saline and phosphate-buffered saline (PBS), and the myocardial tissue in the infarcted area and surrounds was collected. The amount of 4% formalin fixing solution was calculated based on five to 10 times the volume of the samples so that the samples were completely immersed in the fixing solution. After dehydration, transparency and wax dipping, the samples were embedded for slicing.

Haematoxylin staining

Paraffin specimens were sectioned, dewaxed, hydrated and haematoxylin staining drops were added to the sections to cover the tissue evenly. The tissue was then flushed with running water, dipped into 1% hydrochloric acid alcohol, flushed again with running water, stained with eosin, flushed in running water and dehydrated with increasing concentrations of alcohol. Xylene was then used for transparency and neutral resin was used for sealing the tissue sections.

Hematoxylin basic fuchsin picric acid staining

The paraffin specimens were sectioned and routinely dewaxed, stained with aluminum ammonium haematoxylin, washed with 0.1% alkaline fuchsin dye, washed with running water, separated with 0.1% picric acid and acetone, rapidly dehydrated with acetone, made transparent with xylene, and sealed with neutral resin. The normal myocardium appeared yellow, the nucleus was black and the infarcted myocardium was red.

Ten high-magnification samples were randomly selected from each slice ($\times 400$ visual field) and image analysis software Image Pro Plus 6.0 was used for semi-quantitative analysis to detect the average optical density of the 10 selected visual field-positive areas. An average value was taken as the degree of infarction.

Immunohistochemistry

The results of immunohistochemical staining were determined using the immunohistochemical visualisation method. The paraffin specimens were sectioned, dewaxed, hydrated and incubated with 3% H_2O_2 for 30 minutes. A high-pressure heat-repair antigen was added. Primary anti-VEGF (ready-to-use working solution), Beclin1 (1:100), mTOR (1:150) and SIRT1 (1:100) were added dropwise. They were placed in a 4°C refrigerator overnight, then the second antibody was added, and they were then placed in a 37°C incubator for 30 minutes.

DAB staining and haematoxylin re-staining was carried out, 1% hydrochloric acid-ethanol differentiation was done, and bluing, dehydration, transparency and sealing were performed. VEGF, SIRT1, Beclin1 and mTOR were used as positive controls with positive sections of known colorectal cancer, and PBS was used as a negative control instead of the primary antibody.

VEGF, SIRT1, Beclin1 and mTOR were all expressed in the cytoplasm, and the presence of brownish-yellow particles was positive. Ten high-power cells were randomly selected from each section ($\times 400$ of the visual field), and image Pro Plus 6.0 image analysis software was used for semi-quantitative analysis to detect the average optical density of the 10 selected positive areas of the visual field. An average value was taken as its relative expression.

Immunofluorescence staining

Serial sections of rabbit myocardial tissue of 4 μm were cut. After routine dewaxing, dehydration, repair and blocking with foetal sheep serum, mouse anti-human CD31 monoclonal antibody (1:50) was added at 4°C overnight. The next day, after PBS rinsing, Alexa 488 labelled goat anti-mouse IgG (1:400) was added and incubated at 37°C for one hour, and at room temperature for five minutes. The samples were then rinsed with

PBS and the film was sealed and observed under a fluorescence microscope.

Vascular endothelial cells were labelled with CD31, and green cytoplasmic fluorescence was regarded as positive. The criterion for determining microvascular density (MVD) was according to Weidner’s method: under the fibroscope, single endothelial cells, endothelial cell clusters, vessels surrounding the lumen and vessels containing one to two layers of smooth muscle are regarded as microvessels and counted. To determine the MVD value, under the low-power lens ($\times 40$) select the ‘hot spot’ area with the highest density of microvessel distribution and count five high-power microscopic fields (\times the number of microvessels in 200). Take the average value to determine the MVD.

Statistical analysis

SPSS 23.0 software was used to statistically analyse the data measured in the above experiments. The quantitative data are expressed by mean \pm standard deviation. One-way way ANOVA was used for comparisons among groups. The least significant difference (LSD) method was used to compare the two groups. Statistical significance was set at $p < 0.05$.

Results

The ECG of the animal model was recorded with an animal physiological function monitor before and after ligation of the anterior descending branch of the left coronary artery. The ST-segment was significantly elevated after ligation of the anterior descending branch, which indicated that the acute myocardial infarction model was successful, as shown in Fig. 1.

Histological observation of the rabbit myocardium in each group showed that the myocardial fibres of the control and sham operation groups were arranged in an orderly manner, the cell structure was complete, and the nucleus was large and oval.

In the normal saline + AMI group, the myocardial fibres were in disorder, the muscle nucleus had disappeared, there was swelling and vacuolar degeneration of the myocardial cells and neutrophil infiltration in the myocardial interstitium.

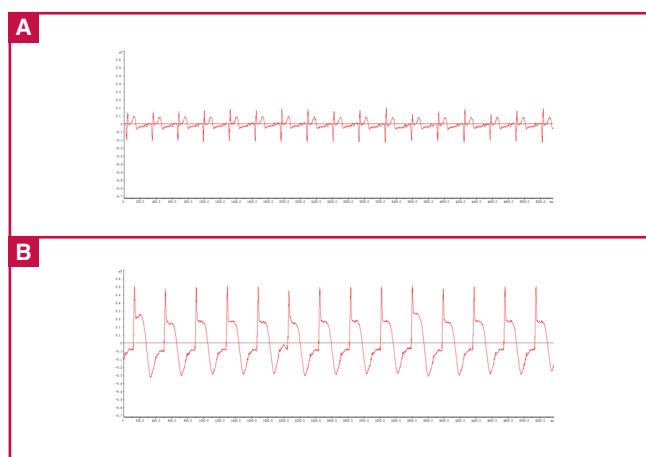


Fig. 1. An ECG judged that the modelling of the acute myocardial infarction model was successful. A. Pre-operative resting ECG; B. ECG after ligation of the anterior descending branch.

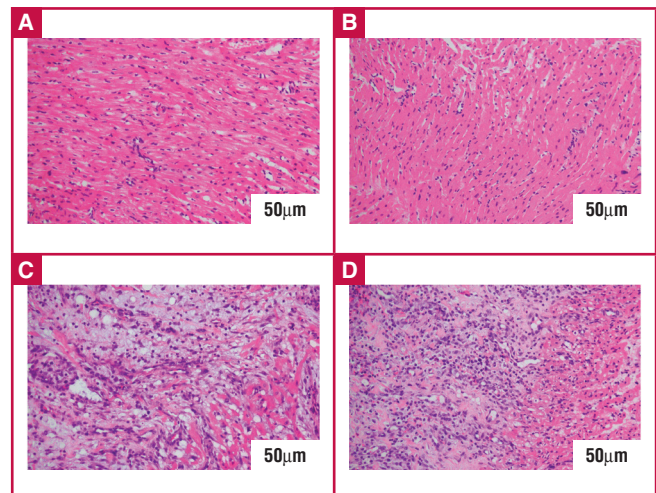


Fig. 2. Comparison of haematoxylin–eosin (HE) staining in the myocardial tissue of rabbits in the control group and in the model groups. A. HE staining in the control group; B. HE staining in the sham operation group; C. HE staining the normal saline + AMI group; D. HE staining in the SBP + AMI group. Representative images are shown at 20×10 magnifications.

In the myocardial tissue of the SBP + AMI group, there were wavy changes in the myocardial fibres, coagulation of the sarcoplasm, proliferation of blood vessels around the infarcted area and organisation could be seen, as shown in Fig. 2.

The results of picric acid staining in each group showed that no obvious infarction was found in the control and sham operation groups, and a large area of myocardial infarction was observed in the normal saline + AMI and SBP + AMI groups. Compared with the normal saline + AMI and SBP + AMI groups, the degree of infarction of the SBP + AMI group was less than that of the normal saline + AMI group, and the difference was statistically significant ($p < 0.05$) (Table 1, Fig. 3).

The results of immunohistochemical staining showed that VEGF, SIRT1, Beclin1 and mTOR were expressed in the myocardium of the four groups, and the brownish-yellow colour in the cytoplasm was positive. Compared with the control group and the sham operation group, the positive expression of VEGF, Beclin1 and mTOR were significantly increased in the normal saline + AMI group and the SBP + AMI group, while the expression of SIRT1 was decreased. Compared with the normal saline + AMI group, the positive expression of VEGF, Beclin1, mTOR and SIRT1 in the SBP + AMI group was significantly increased ($p < 0.05$), and the difference was statistically significant, as shown in Table 2 and Fig. 4.

The expression of CD31 in each group was marked by immunofluorescence and the MVD values of each group were

Table 1. Mean optical density of picric acid staining results (mean \pm SD)

| | Control group | Sham operation group | Normal saline + AMI group | SBP + AMI group | F-value | p-value |
|---------------|---------------------|----------------------|---------------------------|----------------------------------|---------|---------|
| Staining area | 0.2056 \pm 0.0479 | 0.2169 \pm 0.0503 | 0.5547 \pm 0.0735* | 0.4798 \pm 0.0919 [#] | 68.865 | < 0.001 |

*Compared with the control group and sham operation group, the difference was statistically significant. [#]Compared with normal saline + AMI group, the difference was statistically significant.

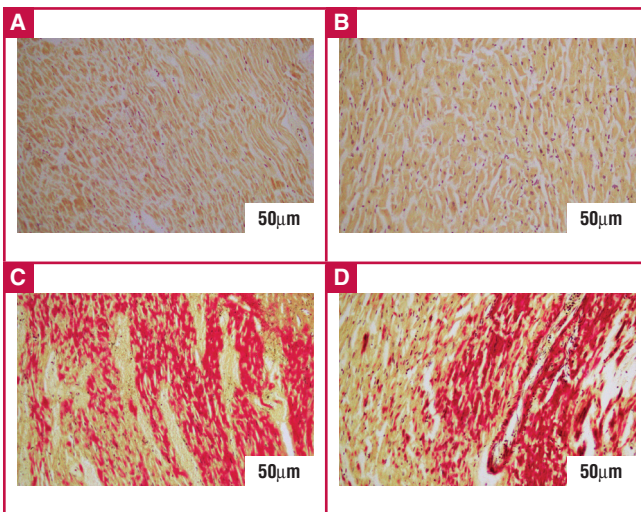


Fig. 3. Comparison of picric acid staining in myocardial tissues of rabbits in the control group and in the model groups. A. Picric acid staining in the control group; B. Picric acid staining in the sham operation group; C. Picric acid staining in the normal saline + AMI group; D. Picric acid staining in the SBP + AMI group. Representative images are shown at 20×10 magnifications.

counted. The results showed that compared with the control and sham operation groups, MVD in the ischaemic area of the normal saline + AMI and SBP + AMI groups increased significantly ($p < 0.05$). Compared with the normal saline + AMI group, MVD in the ischaemic area of the SBP + AMI group was higher than that of the normal saline + AMI group ($p < 0.05$). These differences were statistically significant, as shown in Table 2 and Fig. 5.

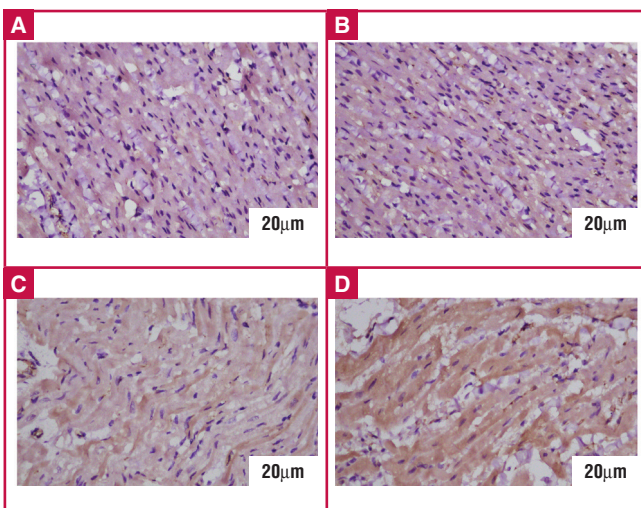


Fig. 4.1. Protein expression levels of VEGF in myocardial tissue by immunohistochemistry staining. A. Immunohistochemistry staining of VEGF in the control group; B. Immunohistochemistry staining of VEGF in the sham operation group; C. Immunohistochemistry staining of VEGF in the normal saline + AMI group; D. Immunohistochemistry staining of VEGF in the SBP + AMI group. Representative images are shown at 20×10 magnifications.

Table 2. Mean optical density of VEGF, Beclin1 and MVD expression in rabbit myocardium (mean \pm SD)

| Groups | VEGF | Beclin1 | MVD |
|---------------------|-----------------------|-----------------------|-------------------|
| Control | 0.1204 \pm 0.0347 | 0.1305 \pm 0.0374 | 5.80 \pm 2.04 |
| Sham operation | 0.1445 \pm 0.0361 | 0.1213 \pm 0.0272 | 6.00 \pm 1.41 |
| Normal saline + AMI | 0.2789 \pm 0.0683* | 0.2583 \pm 0.0577* | 21.4 \pm 4.32* |
| SBP + AMI | 0.3584 \pm 0.0594** | 0.3314 \pm 0.0820** | 25.9 \pm 6.52** |
| F-value | 47.478 | 34.179 | 64.515 |
| p-value | < 0.001 | < 0.001 | < 0.001 |

*Compared with the control and sham operation groups, the difference was statistically significant. **Compared with the normal saline + AMI group, the difference was statistically significant.

Discussion

The process of angiogenesis refers to the original capillaries, under the control of a variety of angiogenic factors, such as VEGF and basic fibroblast growth factor (bFGF), which cause vascular endothelial cells to proliferate and migrate continuously, and finally form new capillary vessels. Therapeutic angiogenesis involves the use of angiogenesis-inducing factors to induce angiogenesis in or around the ischaemic myocardium and promote the formation of collateral circulation.

Many drugs and methods have been used to promote angiogenesis.^{5,6} Studies have shown that SBP can improve the function of the vascular endothelium and myocardial perfusion, promote therapeutic angiogenesis, prevent the pathological progression of coronary heart disease, and improve the long-term prognosis of patients.^{2,7} Zhang *et al.* reported that SBP can promote angiogenesis by activating macrophages to regulate endothelial cell function and signal transduction pathways.⁸ It was found in a rat model of myocardial infarction that SBP could promote angiogenesis in the infarct margin and improve cardiac function.⁹

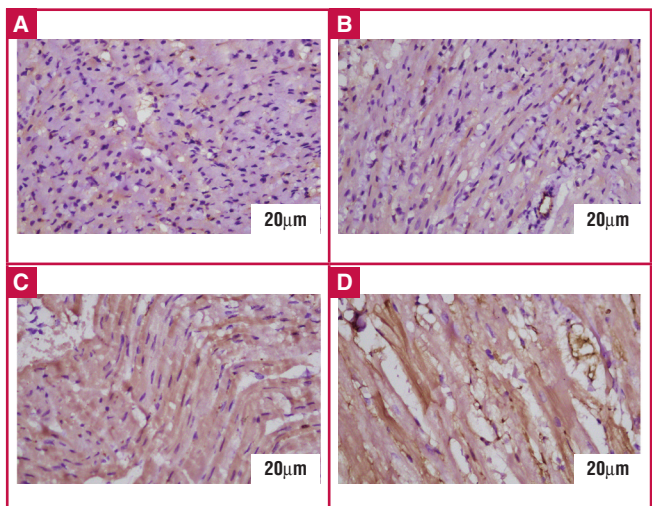


Fig. 4.2. Protein expression levels of Beclin1 in myocardial tissue by immunohistochemistry staining. A. Immunohistochemistry staining of Beclin1 in the control group; B. Immunohistochemistry staining of Beclin1 the sham operation group; C. Immunohistochemistry staining of Beclin1 in the normal saline + AMI group; D. Immunohistochemistry staining of Beclin1 in the SBP + AMI group. Representative images are shown at 20×10 magnifications.

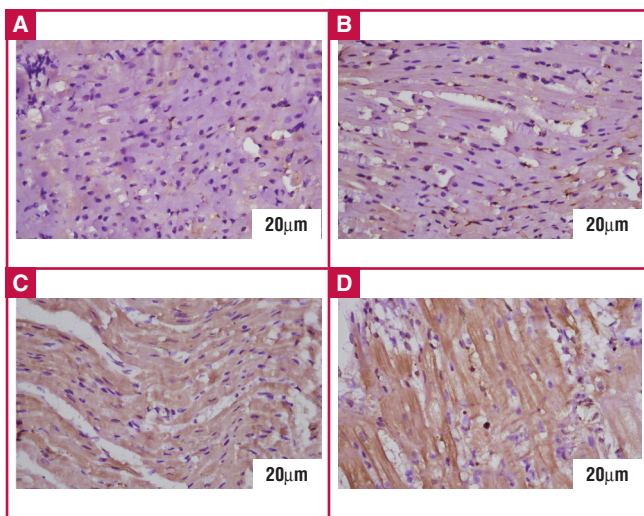


Fig. 4.3. Protein expression levels of mTOR in myocardial tissue by immunohistochemistry staining. A. Immunohistochemistry staining of mTOR in the control group; B. Immunohistochemistry staining of Beclin1 in the sham operation group; C. Immunohistochemistry staining of mTOR in the normal saline + AMI group; D. Immunohistochemistry staining of mTOR in the SBP + AMI group. Representative images are shown at 20 × 10 magnifications.

In this study, an acute myocardial infarction model was established by ligating the anterior descending branch of the left coronary artery, and an animal physiological function monitor was used to confirm the success of the model. Then the SBP was administered and the expression of VEGF in myocardial tissue was determined. The results showed that compared with the normal saline + AMI group, the expression of VEGF in the SBP + AMI group was significantly increased, and the expression of CD31 was significantly increased. It can be seen that SBP participated in angiogenesis after acute myocardial infarction, so it is worth further study to see whether SBP participates in angiogenesis after acute myocardial infarction.

Autophagy involves the use of lysosomes to phagocytise aging organelles, proteins and other macromolecules. It helps to maintain the balance of intracellular protein metabolism and the stability of the internal environment.¹⁰ The autophagy-associated gene (ATG) is required to participate in the process of autophagy. Beclin1, a characteristic protein of autophagy, promotes autophagy. Beclin1 induces autophagosome formation and the autophagy process under conditions of malnutrition, inflammatory stimulation or reactive oxygen species stress.¹¹

Zou *et al.* found that both Beclin1 small interfering RNA and 3-methyladenine treatment predominantly mitigated VEGF-A-induced tube formation and migration of human umbilical vein endothelial cells.¹² In the process of wound healing, local tissue hypoxia and low perfusion injury will induce autophagy, which promotes the growth of endothelial cells and the regeneration of wound microvessels.¹³ mTOR can centrally regulate autophagy. When nutrition is abundant, mTOR complex 1 (mTORC1) can integrate cell signals such as growth factors, energy status, oxygen content and amino acids to promote anabolism, block catabolism, and promote cell growth and proliferation.¹⁴

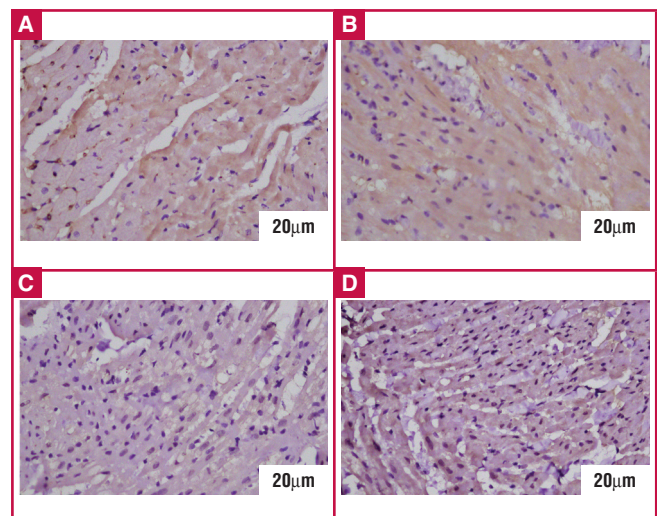


Fig. 4.4. Protein expression levels of SIRT1 in myocardial tissue by immunohistochemistry staining. A. Immunohistochemistry staining of SIRT1 in the control group; B. Immunohistochemistry staining of SIRT1 the sham operation group; C. Immunohistochemistry staining of SIRT1 in the normal saline + AMI group; D. Immunohistochemistry staining of SIRT1 in the SBP + AMI group. Representative images are shown at 20 × 10 magnifications.

In this study, compared with the control and the sham operation groups, expression of Beclin1 increased in the normal saline + AMI group and the SBP + AMI group, and autophagy occurred during the process of acute myocardial infarction. Compared to the normal saline + AMI and SBP + AMI groups, the expression of Beclin1, mTOR, and VEGF increased in the SBP + AMI group. Studies have shown that mTOR activation promotes the production of VEGF, which is an important

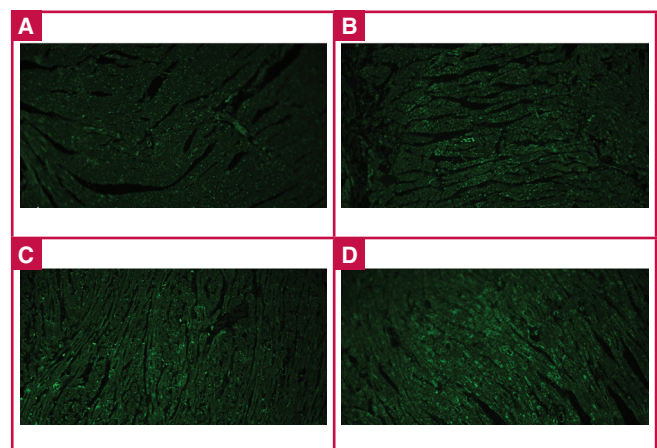


Fig. 5. Assessment of microvessel density (MVD) in myocardial tissue by immunofluorescence staining of CD31. A. immunofluorescence staining of CD31 in the control group; B. Immunofluorescence staining of CD31 in the sham operation group; C. Immunofluorescence staining of CD31 in the normal saline + AMI group; D. Immunofluorescence staining of CD31 in the SBP + AMI group. Representative images are shown at 20 × 10 magnifications.

nutritional factor for angiogenesis and can effectively promote tissue angiogenesis after ischaemia and hypoxia.¹⁵ We believe that after acute myocardial infarction, the activation of mTOR may promote the expression of VEGF in the myocardial tissue of acute myocardial infarction and effectively promote angiogenesis.

As a deacetylase, SIRT1 plays an important role in many processes, such as the inflammatory response, cell apoptosis and proliferation by regulating the deacetylation of related proteins.¹⁶ Kilic *et al.* showed that the cardiovascular risk sites rs7069102 and rs2273773 of SIRT1 may participate in the occurrence and development of acute myocardial infarction by regulating the expression of SIRT1 and eNOS in myocardial tissue.¹⁷

Chan *et al.* proposed for the first time that inhibition of SIRT1 activity can cause cardiac oxidative stress and inflammatory responses, leading to coronary atherosclerotic heart disease. Activation of SIRT1 function can reverse coronary atherosclerosis.¹⁸ Potente *et al.* showed that compared to the myocardium of normal mice, the myocardial infarction area of SIRT1 knockout mice was significantly increased, but the infarct size of SIRT1 overexpression mice was significantly smaller than that of normal mice.¹⁹

In this study, compared with the control and sham operation groups, the expression of SIRT1 decreased significantly in the normal saline + AMI and SBP + AMI groups. It can be seen that the expression of SIRT1 decreased during the occurrence of acute myocardial infarction. Compared with the normal saline + AMI and SBP + AMI groups, the myocardial infarction area of the SBP + AMI group decreased, and the expression of SIRT1 increased. Therefore, we believe that SIRT1 may play a positive regulatory role in the treatment of acute myocardial infarction with SBP protecting the myocardial cells. However, its regulatory mechanism is not clear.

Increasing evidence shows that the SIRT1/mTOR signalling pathway plays a key role in cardiovascular diseases.²⁰ SIRT1 can regulate autophagy-related genes and activate autophagy through deacetylation, playing a positive regulatory role in autophagy.²¹ SIRT1 is closely related to autophagy. In starvation and other energy-deficiency states, the NAD⁺ content increases to activate the SIRT1 pathway. It directly deacetylates and activates autophagy by forming a complex with autophagy-related genes *ATG5*, *Atg7* and *Atg8*, or induces autophagy by activating FOXO.²² Luo also suggested that Sirt1 promoted autophagy via AMPK activation.²³

In this study, the expression of SIRT1, Beclin1, mTOR and VEGF increased significantly in the SBP + AMI group. We speculate that after acute myocardial infarction, due to the SBP, the SIRT1 pathway is activated, leading to deacetylation of Beclin1 and activation of autophagy, thereby negatively regulating mTOR through feedback. This then promotes the expression of VEGF factor in the myocardial tissue after acute myocardial infarction, promoting angiogenesis and accelerating the formation of collateral circulation. However, the target of the SIRT1/mTOR signalling pathway in angiogenesis after acute myocardial infarction remains unclear and requires further research.

Conclusion

In this study, SBP was administered to rabbits after acute myocardial infarction. From the determination of related factors, the results showed that SBP promoted angiogenesis after acute

myocardial infarction through the SIRT1/mTOR signalling pathway, enhanced the formation of collateral circulation, and was of great significance in restoring blood supply to the ischaemic myocardium. However, the specific site of action of the SBP is still unclear and needs to be further studied and verified at the cell level.

This study was funded by the Science and Technology Project of the Binzhou Medical University (grant no. BY2017KJ16) and the China Association of Integrated Chinese and Western Medicine Scientific Research Fund Project (grant no. 2018010).

References

- Zhang N, Chen J, Song YN. Research progress on promoting coronary microcirculation angiogenesis after myocardial infarction. *Zhong Hua Xin Xue Guan Bing Za Zhi* 2018; **46**(10): 828–830.
- Ke-Jian Zhang, Jia-Zhen Zhu, Xiao-Yi Bao, Qun Zheng, Guo-Qing Zheng, Yan Wang. Shexiang Baoxin pills for coronary heart disease in animal models: preclinical evidence and promoting angiogenesis mechanism. *Front Pharmacol* 2017; **8**: 404.
- Mengxi Wang, Yiwen Shan, Weixin Sun, Jie Han, Huaqin Tong, Manlu Fan, *et al.* Effects of Shexiang Baoxin pill for coronary microvascular function: a systematic review and meta-analysis. *Front Pharmacol* 2021; **12**: 751050.
- Xing Yuan, Lin Han, Peng Fu, Huawu Zeng, Chao Lv, Wanlin Chang, *et al.* Cinnamaldehyde accelerates wound healing by promoting angiogenesis via up-regulation of PI3K and MAPK signaling pathways. *Lab Invest* 2018; **98**(6): 783–798.
- M A Schreve, C G Vos, A C Vahl, J P P M de Vries, S Kum, G J de Borst, *et al.* Venous arterialisation for salvage of critically ischaemic limbs: a systematic review and meta-analysis. *Eur J Vasc Endovasc Surg* 2017; **53**(3): 387–402.
- Xiyang Yang, Xingbing Li, Minghao Luo, Yongzheng Guo, Chang Li, Dingyi Lv, *et al.* Tubeimoside I promotes angiogenesis via activation of eNOS-VEGF signaling pathway. *J Ethnopharmacol* 2021; **267**: 113642.
- Hu J, Zhao Y, Wu Y, Yang K, Hu K, Sun A, *et al.* Shexiang Baoxin pill attenuates ischemic injury by promoting angiogenesis by activation of aldehyde dehydrogenase 2. *Cardiovasc Pharmacol* 2021; **77**(3): 408–417.
- Zhang J, Cui Q, Zhao Y, Guo R, Zhan C, Jiang P, *et al.* Mechanism of angiogenesis promotion with Shexiang Baoxin pills by regulating function and signaling pathway of endothelial cells through macrophages. *Atherosclerosis* 2020; **292**: 99–111.
- Lu L, Sun X, Chen C, Qin Y, Guo X. Shexiang Baoxin pill, derived from the traditional Chinese medicine, provides protective roles against cardiovascular diseases. *Front Pharmacol* 2018; **9**: 1161.
- Liu N, Shi Y, Zhuang S. Autophagy in chronic kidney diseases. *Kidney Dis* 2016; **2**(1): 37–45.
- Guoping Shi, Dan Li, Jing Ren, Xiaojing Li, Tingting Wang, Huan Dou, *et al.* mTOR inhibitor INK128 attenuates dextran sodium sulfate-induced colitis by promotion of MDSCs on Treg cell expansion. *J Cell Physiol* 2018; **234**(2): 1618–1629.
- Zou J, Fei Q, Xiao H, Wang H, Liu K, Liu M, *et al.* VEGF-A promotes angiogenesis after acute myocardial infarction through increasing ROS production and enhancing ER stress-mediated autophagy. *Cell Physiol* 2019; **234**(10): 17690–17703.
- Chen Y, Yan Q, Xu Y, Ye F, Sun X, Zhu H, *et al.* NIP3-mediated autophagy induced inflammatory response and inhibited VEGF expression in cultured retinal pigment epithelium cells under hypoxia. *Curr Mol Med* 2019; **19**(6): 395–404.

14. Haojie Wang, Yumei Liu, Dongmei Wang, Yaolu Xu, Ruiqi Dong, Yuxiang Yang, *et al.* The upstream pathway of mTOR-mediated autophagy in liver diseases. *Cells* 2019; **8**(12): 1597.
 15. Hongju Chen, Tao Xiong, Yi Qu, Fengyan Zhao, Donna Ferriero, Dezhi Mu. mTOR activate shypoxia inducible factor 1 α and inhibits neuronal apoptosis in the developing rat brain in during the early phase after hypoxia ischemia. *Neurosci Lett* 2012; **507**(2): 118–123.
 16. Alves-Fernandes DK, Jasiulionis MG. The role of SIRT1 on DNA damage response and epigenetic alterations in cancer. *Int J Mol Sci* 2019; **20**(13): 3153.
 17. Kilic U, Gok O, Bacaksiz A, Izmirli M, Elibol-Can B, Uysal O. SIRT1 gene polymorphisms affect the protein expression in cardiovascular diseases. *PLoS One* 2014; **9**(2): e90428.
 18. Chan SH, Hung CH, Shih JY, Chu PM, Cheng YH, Lin HC, *et al.* SIRT1 inhibition causes oxidative stress and inflammation in patients with coronary artery disease. *Redox Biol* 2017; **13**: 301–309.
 19. Potente M, Ghaeni L, Baldessari D, Mostoslavsky R, Rossig L, Dequiedt F, *et al.* SIRT1 controls endothelial angiogenic functions during vascular growth. *Genes Dev* 2007; **21**(20): 2644–2658.
 20. Peng Yan, Liangjie Bai, Wei Lu, Yuzhong Gao, Yunlong Bi, Gang Lv. Regulation of autophagy by AMP-activated protein kinase/sirtuin 1 pathway reduces spinal cord neurons damage. *Iran J Basic Med Sci* 2017; **20**(9): 1029–1036.
 21. Zhiya Deng, Maomao Sun, Jie Wu, Haihong Fang, Shumin Cai, Sheng An, *et al.* SIRT1 attenuates sepsis-induced acute kidney injury via Beclin1 deacetylation-mediated autophagy activation. *Cell Death Dis* 2021; **12**(2): 217.
 22. Ng F, Tang BL. Sirtuins' modulation of autophagy. *Cell Physiol* 2013; **228**(12): 2262–2270.
 23. Luo G, Jian Z, Zhu Y, Zhu Y, Chen B, Ma R, *et al.* Sirt1 promotes autophagy and inhibits apoptosis to protect cardiomyocytes from hypoxic stress. *Int. J. Mol Med* 2019; **43**(5): 2033–2043.
-